

1

Robust estimation of sulcal morphology

2

Christopher R. Madan

3

School of Psychology

4

University of Nottingham

5

Nottingham, United Kingdom

6

7

Corresponding author:

8

Christopher R. Madan

9

School of Psychology, University of Nottingham

10

Nottingham, NG7 2RD, United Kingdom

11

christopher.madan@nottingham.ac.uk

12 Abstract

13 While it is well established that cortical morphology differs in relation to a variety of
14 inter-individual factors, it is often characterized using estimates of volume, thickness,
15 surface area, or gyrification. Here we developed a computational approach for
16 estimating sulcal width and depth that relies on cortical surface reconstructions output
17 by FreeSurfer. While other approaches for estimating sulcal morphology exist, studies
18 often require the use of multiple brain morphology programs that have been shown to
19 differ in their approaches to localize sulcal landmarks, yielding morphological
20 estimates based on inconsistent boundaries. To demonstrate the approach, sulcal
21 morphology was estimated in three large sample of adults across the lifespan, in
22 relation to aging. A fourth sample is additionally used to estimate test-retest reliability
23 of the approach. This toolbox is now made freely available as supplemental to this
24 paper: <https://cmadan.github.io/calcSulc/>.

25

26 **Keywords:** sulcal width; sulcal depth; age; cortical structure; atrophy; gyrification;
27 cerebral sulci

28 Robust estimation of sulcal morphology

29 **1 Introduction**

30 Cortical structure differs between individuals. It is well known that cortical thickness
31 generally decreases with age (Fjell et al., 2009; Hogstrom et al., 2013; Hutton et al., 2009;
32 Lemaitre et al., 2012; Madan & Kensinger, 2016, 2018; McKay et al., 2014; Salat et al.,
33 2004; Sowell et al., 2003, 2007); however, a more visually prominent difference is the
34 widening of sulci, sometimes described as “sulcal prominence” (Coffey et al., 1992;
35 Drayer, 1988; Jacoby et al., 1980; Laffey et al., 1984; Tomlinson et al., 1968; Yue et al.,
36 1997). In the literature, this measure has been referred to using a variety of names,
37 including sulcal width, span, dilation, and enlargement, as well as fold opening. With
38 respect to aging and brain morphology, sulcal width has been assessed qualitatively by
39 clinicians as an index of cortical atrophy (Coffey et al., 1992; Drayer, 1988; Laffey et al.,
40 1984; Pasquier et al., 1996; Scheltens et al., 1997; Tomlinson et al., 1968). An illustration
41 of age-related differences in sulcal morphology is shown in Figure 1.

42 Using quantitative approaches, sulcal width has been shown to increase with age
43 (Kochunov et al., 2005, 2008; Liu et al., 2010, 2013) likely relating to subsequent
44 findings of age-related decreases in cortical gyrification (Cao et al., 2017; Hogstrom et
45 al., 2013; Madan & Kensinger, 2016, 2018; Madan, 2018a). Sulcal widening has also
46 been shown to be associated with decreases in cognitive abilities (Liu et al., 2011) and
47 physical activity (Lamont et al., 2014). With respect to clinical conditions, increased
48 sulcal width has been found in dementia patients relative to healthy controls
49 (Andersen et al., 2015; Hamelin et al., 2015; Huckman et al., 1975; Liu et al., 2012; Ming
50 et al., 2015; Plochanski & Østergaard, 2016; Reiner et al., 2012), as well as with
51 schizophrenia patients (Largen et al., 1984; Palaniyappan et al., 2015; Rieder et al., 1979)
52 and mood disorders (Elkis et al., 1995).

53 One of the most common programs for conducting cortical surface analyses is
54 FreeSurfer (Fischl, 2012). Unfortunately, though FreeSurfer reconstructs cortical
55 surfaces, it does not estimate sulcal width or depth, leading researchers to use

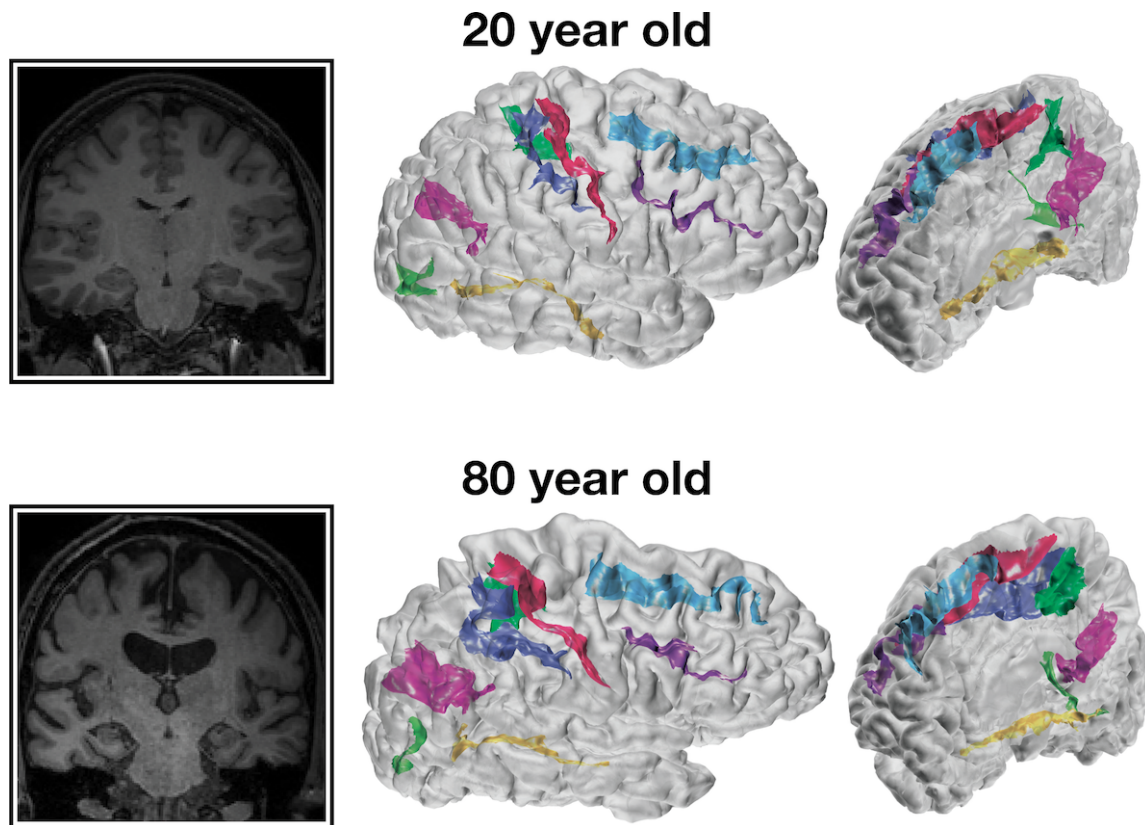


Figure 1. Representative coronal slices and cortical surfaces with sulcal identification for 20- and 80-year-old individuals.

56 FreeSurfer along with another surface analysis program, BrainVISA (Kochunov et al.,
57 2012; Mangin, Rivière, et al., 2004; Mangin, Riviere, et al., 2004; Rivière et al., 2002), to
58 characterize cortical thickness along with sulcal morphology (e.g. Cai et al., 2017;
59 Lamont et al., 2014; Liu et al., 2011, 2013; Pizzagalli et al., 2017). While this combination
60 allows for the estimation of sulcal morphology in addition to standard measures such
61 as cortical thickness, FreeSurfer and BrainVISA rely on different anatomical landmarks
62 (Mikhael et al., 2018) which can yield differences in their resulting cortical surface
63 reconstructions (Lee et al., 2006). Admittedly, determining the boundaries for an
64 individual sulcus and incorporating individual cortical variability is difficult (John et
65 al., 2006; Mikhael et al., 2018; Ono et al., 1990; Welker, 1990). While an ennumerate
66 amount of other methods have already been proposed to identify and characterize
67 sulcal morphology (e.g., Andreasen et al., 1994; Auzias et al., 2015; Beeston & Taylor,
68 2000; Behnke et al., 2003; Eskildsen et al., 2005; Im et al., 2010; Jones et al., 2000; Le

69 Goualher et al., 1996, 1998; Li et al., 2008; Lohmann & von Cramon, 2000; Lohmann et
70 al., 2008; Nowinski et al., 1996; Oguz et al., 2008; Perrot et al., 2011; Royackkers et al.,
71 1999; Thompson et al., 1996; Vaillant & Davatzikos, 1997; Yun et al., 2013), ultimately
72 these all are again using different landmarks than FreeSurfer uses for cortical
73 parcellations (i.e., volume, thickness, surface area, gyrification). Note that, though
74 FreeSurfer itself does compute sulcal maps, these are computed as normalized depths,
75 not in real-world units (e.g. Kippenhan et al., 2005), furthermore, these are also
76 independent of sulcal width information.

77 Here we describe a procedure for estimating sulcal morphology and report
78 age-related differences in sulcal width and depth using three large samples of adults
79 across the lifespan: two of these datasets are from Western samples, Dallas Lifespan
80 Brain Study (DLBS) and Open Access Series of Imaging Studies (OASIS), as well as one
81 East Asian sample, Southwest University Adult Lifespan (SALD), as potential
82 differences between populations have been relatively understudied (Leong et al., 2017;
83 Madan, 2017). To further validate the method, test-retest reliability was also assessed
84 using a sample of young adults who were scanned ten times within the span of a
85 month (Chen et al., 2015; Madan & Kensinger, 2017b). All four of these datasets are
86 open-access and have sufficient sample sizes to be suitable for brain morphology
87 research (Madan, 2017). This procedure has been implemented as a MATLAB toolbox,
88 `calcSulc`, that calculates sulcal morphology—both width and depth—using files
89 generated as part of the standard FreeSurfer cortical reconstruction and parcellation
90 pipeline. This toolbox is now made freely available as supplemental to this paper:
91 <https://cmadan.github.io/calcSulc/>.

92 **2 Materials and Methods**

93 **2.1 Datasets**

94 **OASIS.** This dataset consisted of 314 healthy adults (196 females), aged 18–94, from
95 the Open Access Series of Imaging Studies (OASIS) cross-sectional dataset

96 (<http://www.oasis-brains.org>) (Marcus et al., 2007). Participants were
97 recruited from a database of individuals who had (a) previously participated in MRI
98 studies at Washington University, (b) were part of the Washington University
99 Community, or (c) were from the longitudinal pool of the Washington University
100 Alzheimer Disease Research Center. Participants were screened for neurological and
101 psychiatric issues; the Mini-Mental State Examination (MMSE) and Clinical Dementia
102 Rating (CDR) were administered to participants aged 60 and older. To only include
103 healthy adults, participants with a CDR above zero were excluded; all remaining
104 participants scored 25 or above on the MMSE. Multiple T1 volumes were acquired
105 using a Siemens Vision 1.5 T with a MPRAGE sequence; only the first volume was used
106 here. Scan parameters were: TR=9.7 ms; TE=4.0 ms; flip angle=10°;
107 voxel size=1.25×1×1 mm. Age-related comparisons for volumetric and fractal
108 dimensionality measures from the OASIS dataset were previously reported in Madan
109 and Kensinger (2017a), Madan and Kensinger (2018), and Madan (2018b)¹.

110 **DLBS.** This dataset consisted of 315 healthy adults (198 females), aged 20–89, from
111 wave 1 of the Dallas Lifespan Brain Study (DLBS), made available through the
112 International Neuroimaging Data-sharing Initiative (INDI) (Mennes et al., 2013) and
113 hosted on the Neuroimaging Informatics Tools and Resources Clearinghouse (NITRC)
114 (Kennedy et al., 2016)
115 (http://fcon_1000.projects.nitrc.org/indi/retro/dlbs.html).
116 Participants were screened for neurological and psychiatric issues. No participants in
117 this dataset were excluded *a priori*. All participants scored 26 or above on the MMSE.
118 T1 volumes were acquired using a Philips Achieva 3 T with a MPRAGE sequence. Scan
119 parameters were: TR=8.1 ms; TE=3.7 ms; flip angle=12°; voxel size=1×1×1 mm. See
120 Kennedy et al. (2015) and Chan et al. (2014) for further details about the dataset.
121 Age-related comparisons for volumetric and fractal dimensionality measures from the
122 DLBS dataset were previously reported in Madan and Kensinger (2017a), Madan and

¹Note that analyses reported in these previous papers were based on preprocessing in FreeSurfer 5.3.0, rather than FreeSurfer 6.0.

123 Kensinger (2018), and Madan (2018b) ¹.

124 **SALD.** This dataset consisted of 483 healthy adults (303 females), aged 19–80, from
125 the Southwest University Adult Lifespan Dataset (SALD) (Wei et al., 2018), also made
126 available through INDI and hosted on NITRC
127 (http://fcon_1000.projects.nitrc.org/indi/retro/sald.html). No
128 participants in this dataset were excluded *a priori*. T1 volumes were acquired using a
129 Siemens Trio 3 T with a MPRAGE sequence. Scan parameters were: TR=1.9 s;
130 TE=2.52 ms; flip angle=9°; voxel size=1×1×1 mm.

131 **CCBD.** This dataset consisted of 30 healthy adults (15 females), aged 20–30, from the
132 Center for Cognition and Brain Disorders (CCBD) at Hangzhou Normal University
133 (Chen et al., 2015). Each participant was scanned for 10 sessions, occurring 2-3 days
134 apart over a one-month period. No participants in this dataset were excluded *a priori*.
135 T1 volumes were acquired using a SCANNER with a FSPGR sequence. Scan
136 parameters were: TR=8.06 ms; TE=3.1 ms; flip angle=8°; voxel size: 1×1×1 mm. This
137 dataset is included as part of the Consortium for Reliability and Reproducibility
138 (CoRR) (Zuo et al., 2014) as HNU1. Test-retest comparisons for volumetric and fractal
139 dimensionality measures from the CCBD dataset were previously reported in Madan
140 and Kensinger (2017b)¹.

141 **2.2 Procedure**

142 Data were analyzed using FreeSurfer 6.0
143 (<https://surfer.nmr.mgh.harvard.edu>) on a machine running Red Hat
144 Enterprise Linux (RHEL) 7.4. FreeSurfer was used to automatically volumetrically
145 segment and parcellate cortical and subcortical structures from the T1-weighted
146 images (Fischl, 2012; Fischl & Dale, 2000) FreeSurfer's standard pipeline was used (i.e.,
147 `recon-all`). No manual edits were made to the surface meshes, but surfaces were
148 visually inspected. Cortical thickness is calculated as the distance between the white

149 matter surface (white-gray interface) and pial surface (gray-CSF interface) .
150 Gyrfication was also calculated using FreeSurfer, as described in Schaer et al. (2012).
151 Cortical regions were parcellated based on the Destrieux et al. (2010) atlas, also part of
152 the standard FreeSurfer analysis pipeline.

153 3 Calculation

154 Here we outline a novel, simple yet robust, automated approach for estimating sulcal
155 width and depth, based on intermediate files generated as part of the standard
156 FreeSurfer analysis pipeline. This procedure and functionality has been implemented
157 in an accompanying MATLAB toolbox, `calcSulc`. The toolbox is supplemental
158 material to this paper and is made freely available:
159 <https://cmadan.github.io/calcSulc/>.

160 For each individual sulcus (for each hemisphere and participant), the following
161 approach was used to characterize the sulcal morphology. The procedure has been
162 validated and is supported for the following sulci: central, post-central, superior
163 frontal, inferior frontal, parieto-occipital, occipito-temporal, middle occipital and
164 lunate, and marginal part of the cingulate (`S_central`, `S_postcentral`,
165 `S_front_sup`, `S_front_inf`, `S_parieto_occipital`,
166 `S_oc-temp_med&Lingual`, `S_oc_middle&Lunatus`, `S_cingul-Marginalis`).
167 All of the sulci are labeled in Figure 2.

168 First the pial surface and Destrieux et al. (2010) parcellation labels were read into
169 MATLAB by using the FreeSurfer-MATLAB toolbox provided alongside FreeSurfer
170 (`calcSulc_load`), this consists of the `?h.pial` (FreeSurfer cortical surface mesh)
171 `?h.aparc.a2009s.annot` (FreeSurfer parcellation annotation) files. Using this, the
172 faces associated with the individual sulcus were isolated as a 3D mesh
173 (`calcSulc_isolate`).

174 The width of each sulcus (`calcSulc_width`) was calculated by determining
175 which vertices lay on the boundary of the sulcus and the adjacent gyrus. An iterative
176 procedure was then used to determine the 'chain' of edges that would form a

177 contiguous edge-loop that encircle the sulcal region (`calcSulc_getEdgeLoop`). This
178 provided an exhaustive list of all vertices that were mid-way between the peak of the
179 respective adjacent gyri and depth of the sulcus itself. For each vertex in this edge-loop,
180 the nearest point in 3D space that was *not* neighbouring in the loop was determined,
181 with the goal of finding the nearest vertex in the edge that was on the opposite side of
182 the sulcus—i.e., a line between these two vertices would ‘bridge’ across the sulcus. Since
183 these nearest vertices in the edge loop are not necessarily the nearest vertex along the
184 opposite sulcus wall, an exhaustive search (walk) was performed, moving up to a 4
185 edges from the initially determined nearest vertex (configurable as
186 `options.setWidthWalk`). The sulcal width was then taken as the median of these
187 distances that bridged across the sulcus.

188 The depth of each sulcus (`calcSulc_depth`) additionally used FreeSurfer’s
189 sulcal maps (`?h.sulc`) to determine the relative inflections in the surface mesh, which
190 would be in alignment with the gyral crown. The deepest points of the sulcus, i.e., the
191 sulcal fundus, were taken as the 100 vertices within the sulcus with the lowest values
192 in the sulcal map. For these 100 vertices, the shortest distance to the smoothed
193 enclosing surface was calculated (generated by FreeSurfer’s built-in gyrification
194 analysis [`?h.pial-outer-smoothed`], Schaer et al., 2012), and the median of these
195 was then taken as the sulcal depth.

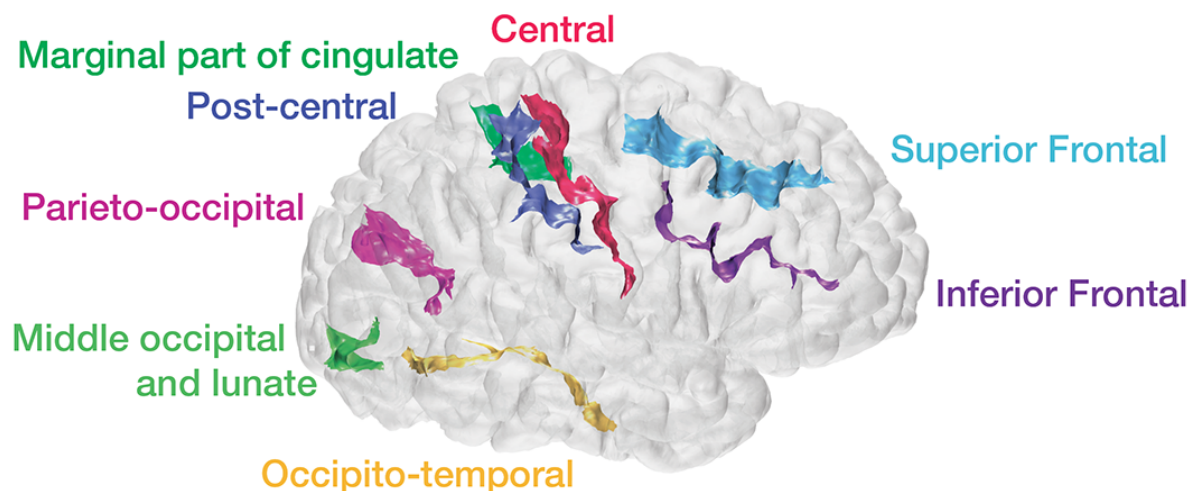


Figure 2. Example cortical surface with estimated sulci identified and labelled.

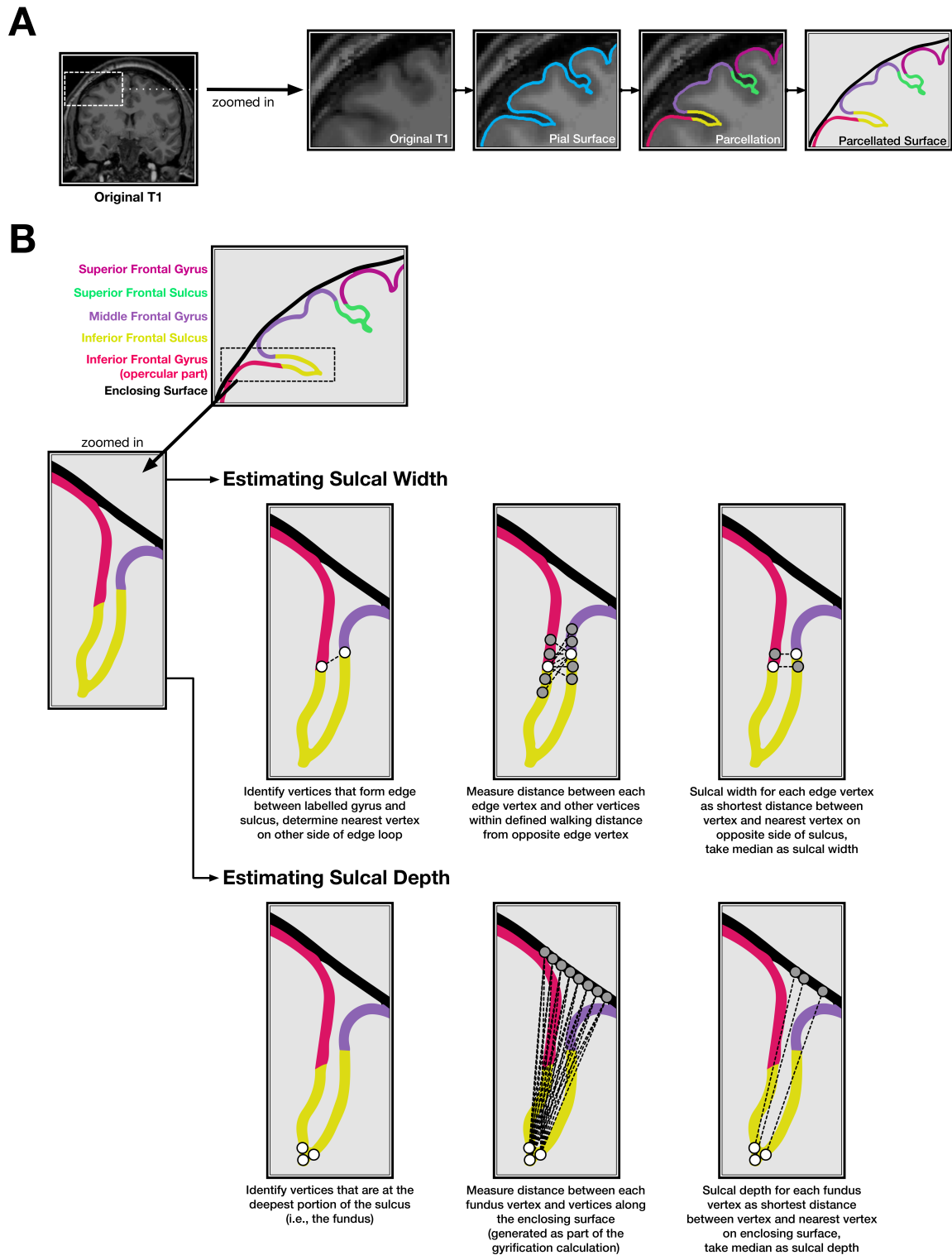


Figure 3. Illustration of the sulcal morphology method. (A) Cortical surface estimation and sulcal identification, as output from FreeSurfer. (B) Sulcal width and depth estimation procedure. Note that the surface mesh and estimation algorithm use many more vertices than shown here.

196 Sulcal morphology, with and depth, was estimated for eight major sulci in each
197 hemisphere: central, post-central, superior frontal, inferior frontal, parieto-occipital,
198 occipito-temporal, middle occipital and lunate, and marginal part of the cingulate
199 (`S_central`, `S_postcentral`, `S_front_sup`, `S_front_inf`,
200 `S_parieto_occipital`, `S_oc-temp_med&Lingual`, `S_oc_middle&Lunatus`,
201 `S_cingul-Marginalis`). Preliminary analyses additionally included superior and
202 inferior temporal sulci and intraparietal sulcus but these were removed from further
203 analysis when the sulci width estimation was found to fail to determine a closed
204 boundary edge-loop at an unacceptable rate ($> 10\%$) for at least one hemisphere. This
205 edge boundary determination failed when parcellated regions were labeled by
206 FreeSurfer to comprise at least two discontinuous regions, such that they could not be
207 identified using a single edge loop. Nonetheless, sulcal measures failed to be estimated
208 for some participants, resulting in final samples of 310 adults from the OASIS dataset,
209 312 adults from the DLBS dataset, 481 adults from the SALD dataset, and 30 adults
210 from the CCBD dataset.

211 3.1 Test-retest reliability

212 Test-retest reliability was assessed as intraclass correlation coefficient (*ICC*), which can
213 be used to quantify the relationship between multiple measurements (Asendorpf &
214 Wallbott, 1979; Bartko, 1966; Chen et al., 2018; Hallgren, 2012; Koo & Li, 2016; Madan &
215 Kensinger, 2017b; Rajaratnam, 1960; Shrout & Fleiss, 1979). McGraw and Wong (1996)
216 provide a comprehensive review of the various *ICC* formulas and their applicability to
217 different research questions. *ICC* was calculated as the one-way random effects model
218 for the consistency of single measurements, i.e., $ICC(1, 1)$. As a general guideline,
219 *ICC* values between .75 and 1.00 are considered 'excellent,' .60-.74 is 'good,' .40-.59 is
220 'fair,' and below .40 is 'poor' (Cicchetti, 1994).

221 4 Results & Discussion

222 4.1 Age-related differences in sulcal morphology

223 Scatter plots showing the relationships between each individual sulcal width and
 224 depth and age, for the OASIS dataset, are shown in Figure 4; the corresponding
 225 correlations for all datasets are shown in Tables 1 and 2. The width and depth of the
 226 central and post-central sulci appear to be particularly correlated with age, with wider
 227 and shallower sulci in older adults. Age-related differences in sulcal width and depth
 228 and generally present in other sulci as well, but are generally weaker.

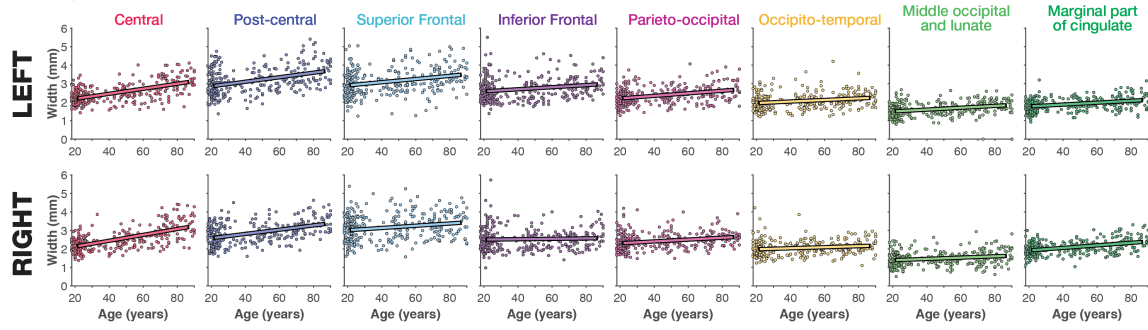
229 Age-related relationships for each sulcus were relatively consistent between the
 230 two Western lifespan datasets (OASIS and DLBS), but age-related differences in sulcal
 231 width (but not depth) were markedly weaker in the East Asian lifespan dataset (SALD).
 232 This finding will need to be studied further, but may be related to gross differences in
 233 anatomical structure (Kochunov et al., 2003; Tang et al., 2010). Importantly, test-retest
 234 reliability, $ICC(1, 1)$, was particularly good for the sulcal depth across individual sulci.

Sulci Name	FreeSurfer Label†	Hemi.	OASIS	DLBS	SALD	CCBD	
			$r(Age)$	$r(Age)$	$r(Age)$	$ICC(1,1)$	95% CI of ICC
Central	S_central	L	.586	.486	.322	.858	[0.785, 0.918]
		R	.632	.523	.294	.842	[0.764, 0.908]
Post-central	S_postcentral	L	.413	.391	.198	.764	[0.660, 0.858]
		R	.460	.436	.213	.864	[0.794, 0.922]
Superior Frontal	S_front_sup	L	.281	.421	.055	.797	[0.703, 0.880]
		R	.205	.291	.035	.843	[0.764, 0.909]
Inferior Frontal	S_front_inf	L	.217	.323	-.037	.775	[0.675, 0.865]
		R	.043	.222	-.036	.831	[0.748, 0.901]
Parieto-occipital	S_parieto_occipital	L	.348	.279	.145	.616	[0.486, 0.753]
		R	.257	.357	.213	.682	[0.561, 0.802]
Occipito-temporal	S_oc-temp_med&Lingual	L	.227	.270	-.055	.660	[0.535, 0.786]
		R	.168	.189	.017	.692	[0.572, 0.808]
Middle occipital and lunate	S_oc_middle&Lunatus	L	.306	.271	.145	.605	[0.474, 0.744]
		R	.212	.177	.023	.625	[0.496, 0.760]
Marginal part of cingulate	S_cingul-Marginalis	L	.340	.275	.075	.783	[0.685, 0.871]
		R	.430	.382	.161	.757	[0.651, 0.853]
<i>Mean</i>			.636	.592	.227	.907	[0.856, 0.947]

Table 1

Correlations between sulcal width and age for each sulci and hemisphere, for each of the three lifespan datasets examined. Test-retest reliability, $ICC(1, 1)$, is also included from the CCBD dataset. †FreeSurfer labels in version 6.0; labels are named slightly different in version 5.3.

A. Sulcal Width



B. Sulcal Depth

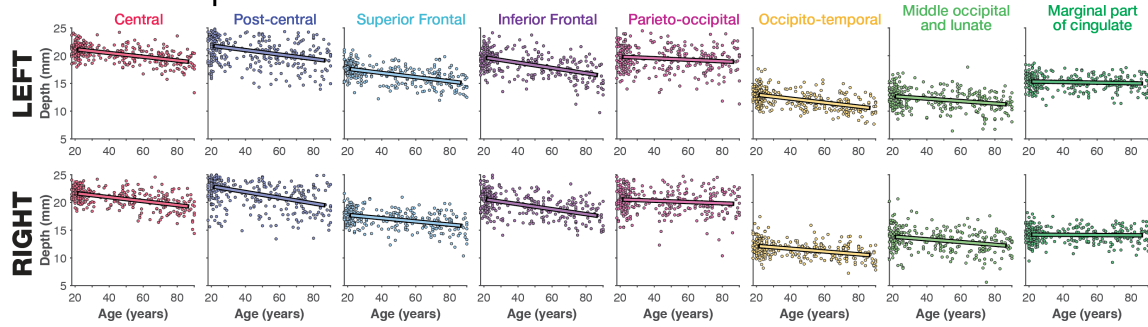


Figure 4. Relationship between (A) sulcal depth and (B) width for each of the sulci examined, based on the OASIS dataset.

Sulci Name	FreeSurfer Label†	Hemi.	OASIS	DLBS	SALD	CCBD	
			$r(\text{Age})$	$r(\text{Age})$	$r(\text{Age})$	$ICC(1,1)$	95% CI of ICC
Central	S_central	L	-.517	-.205	-.346	.848	[0.772, 0.912]
		R	-.505	-.256	-.348	.860	[0.789, 0.919]
Post-central	S_postcentral	L	-.371	-.264	-.268	.965	[0.944, 0.981]
		R	-.436	-.246	-.330	.890	[0.831, 0.937]
Superior Frontal	S_front_sup	L	-.523	-.454	-.397	.899	[0.844, 0.943]
		R	-.413	-.465	-.444	.886	[0.825, 0.935]
Inferior Frontal	S_front_inf	L	-.517	-.490	-.491	.932	[0.893, 0.962]
		R	-.496	-.480	-.490	.915	[0.868, 0.952]
Parieto-occipital	S_parieto_occipital	L	-.145	-.093	-.241	.979	[0.966, 0.989]
		R	-.124	.059	-.229	.970	[0.952, 0.984]
Occipito-temporal	S_oc-temp_med&Lingual	L	-.509	-.323	-.263	.953	[0.926, 0.974]
		R	-.404	-.316	-.281	.913	[0.864, 0.951]
Middle occipital and lunate	S_oc_middle&Lunatus	L	-.290	-.167	-.150	.949	[0.919, 0.972]
		R	-.288	-.120	-.132	.922	[0.879, 0.956]
Marginal part of cingulate	S_cingul-Marginalis	L	-.092	-.035	-.268	.952	[0.925, 0.974]
		R	-.032	-.017	-.156	.918	[0.872, 0.954]
Mean			-.465	-.645	-.600	.972	[0.955, 0.985]

Table 2

Correlations between sulcal depth and age for each sulci and hemisphere, for each of the three lifespan datasets examined. Test-retest reliability, $ICC(1,1)$, is also included from the CCBD dataset. †FreeSurfer labels in version 6.0; labels are named slightly different in version 5.3.

235 To obtain a coarse summary measure across sulci, we averaged the sulcal width
236 across the 16 individual sulci for each individual, and with each dataset, and examined
237 the relationship between mean sulcal width with age. These correlations, shown in
238 Table 1, indicate that the mean sulcal width was generally a better indicator of
239 age-related differences in sulcal morphology than individual sulci, and had increased
240 test-retest reliability. Mean sulcal depth was similarly more sensitive to age-related
241 differences than for an individual sulcus (e.g., it is unclear why the relationship
242 between age and width of the central sulcus differed between samples) and the
243 magnitude of this relationship was more consistent across datasets. Reliability was
244 even higher for mean sulcal depth than mean sulcal width.

245 4.2 Comparison with other age-related structural differences

246 Within each dataset, mean sulcal depth and width correlated with age, as shown in
247 Tables 1 and 2. Of course, other measures of brain morphology also differ with age,
248 such as mean (global) cortical thickness [OASIS: $r(308) = -.793, p < .001$; DLBS:
249 $r(310) = -.759, p < .001$; SALD: $r(479) = -.642, p < .001$]. Additionally, volume of the
250 third ventricle (ICV-corrected) has been previously shown to significantly related to
251 age (Madan & Kensinger, 2017a; Walhovd et al., 2011), and was found to be true in
252 each of the examined lifespan datasets here as well [OASIS: $r(308) = .665, p < .001$;
253 DLBS: $r(310) = .677, p < .001$; SALD: $r(479) = .328, p < .001$]. Previous studies have
254 demonstrated that both of these measures are robust estimates of age-related
255 differences in brain structure.

256 To test if these mean sulcal measures served as distinct measures of age-related
257 differences in brain morphology, beyond those provided by other measures, such as
258 mean cortical thickness and volume of the third ventricle, we conducted partial
259 correlations that controlled for these two other measures of age-related atrophy. Mean
260 sulcal width [OASIS: $r_p(306) = .188, p < .001$; DLBS: $r_p(308) = .177, p = .002$; SALD:
261 $r(477) = .003, p = .96$] and depth [OASIS: $r_p(306) = -.443, p < .001$; DLBS:
262 $r_p(308) = -.397, p < .001$; SALD: $r_p(477) = -.534, p < .001$] both explained unique

263 variance in relation to age. Thus, even though more established measures of
264 age-related differences in brain morphology were replicated here, the additional sulcal
265 measures captured aspects of aging that are not accounted for by these extant
266 measures, indicating that these sulcal measures are worth pursuing further and are not
267 redundant with other measures of brain structure. Providing additional support for
268 this, mean sulcal width and depth were only weakly related to each other [OASIS:
269 $r(308) = -.192, p < .001$; DLBS: $r(310) = .092, p = .104$; SALD: $r(479) = .119, p = .009$].

270 As with the individual sulci measures, we did observe a difference between
271 samples where some age-related measures were less sensitive in the East Asian lifespan
272 sample (SALD), here in the ventricle volume correlation and the unsurprisingly weaker
273 age relationship in the partial correlation using sulcal width. These sample differences
274 are puzzling, though there is a general correspondence between the two Western
275 samples. Given that much of the literature is also based on Western samples, we think
276 further research with East Asian samples, and particularly comparing samples with the
277 same analysis pipeline, is necessary to shed further light on this initial finding.

278 5 Conclusion

279 Differences in sulcal width and depth are quite visually prominent, but are not often
280 quantified when examining individual differences in cortical structure. Here we
281 examined age-related differences in both sulcal measures as a proof-of-principle to
282 demonstrate the utility of the calcSulc toolbox that accompanies this paper and is
283 designed to closely compliment the standard FreeSurfer pipeline. This allows for the
284 additional measurement of sulcal morphology, to add to the extant measures of brain
285 morphology such as cortical thickness, area, and gyrification. Critically, this approach
286 uses the same landmarks and boundaries as in the Destrieux et al. (2010) parcellation
287 atlas, in contrast to all previous approaches to characterize sulcal features. This toolbox
288 is now made freely available as supplemental to this paper:

289 <https://cmadan.github.io/calcSulc/>.

290 Using this approach, here we demonstrate age-related differences in sulcal width

291 and depth, as well as high test-retest reliability. Since individual differences in sulcal
292 morphology are sufficiently distinct from those characterized by other brain
293 morphology measures, this approach should complement extant work of investigating
294 factors that influence brain morphology, e.g., see Figure 3 of Madan and Kensinger
295 (2018). Given the flexibility in the methodological approach, these measures can be
296 readily applied to other samples after being initially processed with FreeSurfer.

297 **Acknowledgments**

298 MRI data used in the preparation of this article were obtained from several sources,
299 data were provided in part by: (1) the Open Access Series of Imaging Studies (OASIS)
300 (Marcus et al., 2007); (2) wave 1 of the Dallas Lifespan Brain Study (DLBS) led by Dr.
301 Denise Park and distributed through INDI (Mennes et al., 2013) and NITRC (Kennedy
302 et al., 2016); (3) the Southwest University Adult Lifespan Dataset (SALD) (Wei et al.,
303 2018), also made available through INDI and hosted on NITRC; and (4) the Center for
304 Cognition and Brain Disorders (CCBD) (Chen et al., 2015) as dataset HNU1 in the
305 Consortium for Reliability and Reproducibility (CoRR) (Zuo et al., 2014).

References

306

- 307 Andersen, S. K., Jakobsen, C. E., Pedersen, C. H., Rasmussen, A. M., Plochanski, M., &
308 Østergaard, L. R. (2015). Classification of Alzheimer's disease from MRI using
309 sulcal morphology. In *Image analysis* (pp. 103–113). Springer International
310 Publishing. doi: 10.1007/978-3-319-19665-7_9
- 311 Andreasen, N. C., Harris, G., Cizadlo, T., Arndt, S., O'Leary, D. S., Swayze, V., & Flaum,
312 M. (1994). Techniques for measuring sulcal/gyral patterns in the brain as
313 visualized through magnetic resonance scanning: BRAINPLOT and BRAINMAP.
314 *Proceedings of the National Academy of Sciences*, 91, 93–97. doi: 10.1073/pnas.91.1.93
- 315
- 316 Asendorpf, J., & Wallbott, H. G. (1979). Maße der Beobachterübereinstimmung: ein
317 systematischer Vergleich. *Zeitschrift für Sozialpsychologie*, 10, 243–252.
- 318 Auzias, G., Brun, L., Deruelle, C., & Coulon, O. (2015). Deep sulcal landmarks:
319 Algorithmic and conceptual improvements in the definition and extraction of
320 sulcal pits. *NeuroImage*, 111, 12–25. doi: 10.1016/j.neuroimage.2015.02.008
- 321 Bartko, J. J. (1966). The intraclass correlation coefficient as a measure of reliability.
322 *Psychological Reports*, 19, 3–11. doi: 10.2466/pr0.1966.19.1.3
- 323 Beeston, C. J., & Taylor, C. J. (2000). Automatic landmarking of cortical sulci. In *Medical*
324 *image computing and computer-assisted intervention—MICCAI 2000* (pp. 125–133).
325 Springer Berlin Heidelberg. doi: 10.1007/978-3-540-40899-4_13
- 326 Behnke, K. J., Rettmann, M. E., Pham, D. L., Shen, D., Resnick, S. M., Davatzikos, C., &
327 Prince, J. L. (2003). Automatic classification of sulcal regions of the human brain
328 cortex using pattern recognition. In M. Sonka & J. M. Fitzpatrick (Eds.), *Medical*
329 *imaging 2003: Image processing*. SPIE. doi: 10.1117/12.480834
- 330 Cai, K., Xu, H., Guan, H., Zhu, W., Jiang, J., Cui, Y., ... Wen, W. (2017). Identification of
331 early-stage Alzheimer's disease using sulcal morphology and other common
332 neuroimaging indices. *PLOS ONE*, 12, e0170875. doi:
333 10.1371/journal.pone.0170875
- 334 Cao, B., Mwangi, B., Passos, I. C., Wu, M.-J., Keser, Z., Zunta-Soares, G. B., ... Soares,

- 335 J. C. (2017). Lifespan gyrification trajectories of human brain in healthy
336 individuals and patients with major psychiatric disorders. *Scientific Reports*, *7*,
337 511. doi: 10.1038/s41598-017-00582-1
- 338 Chan, M. Y., Park, D. C., Savalia, N. K., Petersen, S. E., & Wig, G. S. (2014). Decreased
339 segregation of brain systems across the healthy adult lifespan. *Proceedings of the*
340 *National Academy of Sciences USA*, *111*, E4997–E5006. doi:
341 10.1073/pnas.1415122111
- 342 Chen, B., Xu, T., Zhou, C., Wang, L., Yang, N., Wang, Z., ... Weng, X.-C. (2015).
343 Individual variability and test-retest reliability revealed by ten repeated
344 resting-state brain scans over one month. *PLOS ONE*, *10*, e0144963. doi:
345 10.1371/journal.pone.0144963
- 346 Chen, G., Taylor, P. A., Haller, S. P., Kircanski, K., Stoddard, J., Pine, D. S., ... Cox, R. W.
347 (2018). Intraclass correlation: Improved modeling approaches and applications
348 for neuroimaging. *Human Brain Mapping*, *39*, 1187–1206. doi: 10.1002/hbm.23909
349
- 350 Cicchetti, D. V. (1994). Guidelines, criteria, and rules of thumb for evaluating normed
351 and standardized assessment instruments in psychology. *Psychological Assessment*,
352 *6*, 284–290. doi: 10.1037/1040-3590.6.4.284
- 353 Coffey, C. E., Wilkinson, W. E., Parashos, L., Soady, S., Sullivan, R. J., Patterson, L. J., ...
354 Djang, W. T. (1992). Quantitative cerebral anatomy of the aging human brain: A
355 cross-sectional study using magnetic resonance imaging. *Neurology*, *42*, 527–527.
356 doi: 10.1212/wnl.42.3.527
- 357 Destrieux, C., Fischl, B., Dale, A., & Halgren, E. (2010). Automatic parcellation of
358 human cortical gyri and sulci using standard anatomical nomenclature.
359 *NeuroImage*, *53*, 1–15. doi: 10.1016/j.neuroimage.2010.06.010
- 360 Drayer, B. P. (1988). Imaging of the aging brain. Part I. normal findings. *Radiology*, *166*,
361 785–796. doi: 10.1148/radiology.166.3.3277247
- 362 Elkis, H., Friedman, L., Wise, A., & Meltzer, H. Y. (1995). Meta-analyses of studies of
363 ventricular enlargement and cortical sulcal prominence in mood disorders.

- 364 *Archives of General Psychiatry*, 52, 735. doi: 10.1001/archpsyc.1995.03950210029008
- 365
- 366 Eskildsen, S. F., Uldahl, M., & Ostergaard, L. R. (2005). Extraction of the cerebral
367 cortical boundaries from MRI for measurement of cortical thickness. In
368 J. M. Fitzpatrick & J. M. Reinhardt (Eds.), *Medical imaging 2005: Image processing*.
369 SPIE. doi: 10.1117/12.595145
- 370 Fischl, B. (2012). FreeSurfer. *NeuroImage*, 62, 774–781. doi:
371 10.1016/j.neuroimage.2012.01.021
- 372 Fischl, B., & Dale, A. M. (2000). Measuring the thickness of the human cerebral cortex
373 from magnetic resonance images. *Proceedings of the National Academy of Sciences*
374 *USA*, 97, 11050–11055. doi: 10.1073/pnas.200033797
- 375 Fjell, A. M., Westlye, L. T., Amlie, I., Espeseth, T., Reinvang, I., Raz, N., ... Walhovd,
376 K. B. (2009). High consistency of regional cortical thinning in aging across
377 multiple samples. *Cerebral Cortex*, 19, 2001–2012. doi: 10.1093/cercor/bhn232
- 378 Hallgren, K. A. (2012). Computing inter-rater reliability for observational data: An
379 overview and tutorial. *Tutorials in Quantitative Methods for Psychology*, 8, 23–34.
380 doi: 10.20982/tqmp.08.1.p023
- 381 Hamelin, L., Bertoux, M., Bottlaender, M., Corne, H., Lagarde, J., Hahn, V., ... Sarazin,
382 M. (2015). Sulcal morphology as a new imaging marker for the diagnosis of early
383 onset Alzheimer's disease. *Neurobiology of Aging*, 36, 2932–2939. doi:
384 10.1016/j.neurobiolaging.2015.04.019
- 385 Hogstrom, L. J., Westlye, L. T., Walhovd, K. B., & Fjell, A. M. (2013). The structure of the
386 cerebral cortex across adult life: Age-related patterns of surface area, thickness,
387 and gyrification. *Cerebral Cortex*, 23, 2521–2530. doi: 10.1093/cercor/bhs231
- 388 Huckman, M. S., Fox, J., & Topel, J. (1975). The validity of criteria for the evaluation of
389 cerebral atrophy by computed tomography. *Radiology*, 116, 85–92. doi:
390 10.1148/116.1.85
- 391 Hutton, C., Draganski, B., Ashburner, J., & Weiskopf, N. (2009). A comparison between
392 voxel-based cortical thickness and voxel-based morphometry in normal aging.

- 393 *NeuroImage*, 48, 371–380. doi: 10.1016/j.neuroimage.2009.06.043
- 394 Im, K., Jo, H. J., Mangin, J.-F., Evans, A. C., Kim, S. I., & Lee, J.-M. (2010). Spatial
395 distribution of deep sulcal landmarks and hemispherical asymmetry on the
396 cortical surface. *Cerebral Cortex*, 20, 602–611. doi: 10.1093/cercor/bhp127
- 397 Jacoby, R. J., Levy, R., & Dawson, J. M. (1980). Computed tomography in the elderly: I.
398 The normal population. *British Journal of Psychiatry*, 136, 249–255. doi:
399 10.1192/bjp.136.3.249
- 400 John, J. P., Wang, L., Moffitt, A. J., Singh, H. K., Gado, M. H., & Csernansky, J. G. (2006).
401 Inter-rater reliability of manual segmentation of the superior, inferior and middle
402 frontal gyri. *Psychiatry Research: Neuroimaging*, 148, 151–163. doi:
403 10.1016/j.psychresns.2006.05.006
- 404 Jones, S. E., Buchbinder, B. R., & Aharon, I. (2000). Three-dimensional mapping of
405 cortical thickness using Laplace's equation. *Human Brain Mapping*, 11, 12–32. doi:
406 10.1002/1097-0193(200009)11:1<12::aid-hbm20>3.0.co;2-k
- 407 Kennedy, D. N., Haselgrove, C., Riehl, J., Preuss, N., & Buccigrossi, R. (2016). The
408 NITRC image repository. *NeuroImage*, 124, 1069–1073. doi:
409 10.1016/j.neuroimage.2015.05.074
- 410 Kennedy, K. M., Rodrigue, K. M., Bischof, G. N., Hebrank, A. C., Reuter-Lorenz, P. A.,
411 & Park, D. C. (2015). Age trajectories of functional activation under conditions of
412 low and high processing demands: An adult lifespan fMRI study of the aging
413 brain. *NeuroImage*, 104, 21–34. doi: 10.1016/j.neuroimage.2014.09.056
- 414 Kippenhan, J. S., Olsen, R. K., Mervis, C. B., Morris, C. A., Kohn, P., Meyer-Lindenberg,
415 A., & Berman, K. F. (2005). Genetic contributions to human gyrification: Sulcal
416 morphometry in Williams syndrome. *Journal of Neuroscience*, 25, 7840–7846. doi:
417 10.1523/jneurosci.1722-05.2005
- 418 Kochunov, P., Fox, P., Lancaster, J., Tan, L. H., Amunts, K., Zilles, K., ... Gao, J. H.
419 (2003). Localized morphological brain differences between english-speaking
420 caucasians and chinese-speaking asians: new evidence of anatomical plasticity.
421 *NeuroReport*, 14, 961–964. doi: 10.1097/01.wnr.0000075417.59944.00

- 422 Kochunov, P., Mangin, J.-F., Coyle, T., Lancaster, J., Thompson, P., Rivière, D., . . . Fox,
423 P. T. (2005). Age-related morphology trends of cortical sulci. *Human Brain*
424 *Mapping*, 26, 210–220. doi: 10.1002/hbm.20198
- 425 Kochunov, P., Rogers, W., Mangin, J.-F., & Lancaster, J. (2012). A library of cortical
426 morphology analysis tools to study development, aging and genetics of cerebral
427 cortex. *Neuroinformatics*, 10, 81–96. doi: 10.1007/s12021-011-9127-9
- 428 Kochunov, P., Thompson, P. M., Coyle, T. R., Lancaster, J. L., Kochunov, V., Royall, D.,
429 . . . Fox, P. T. (2008). Relationship among neuroimaging indices of cerebral health
430 during normal aging. *Human Brain Mapping*, 29, 36–45. doi: 10.1002/hbm.20369
- 431 Koo, T. K., & Li, M. Y. (2016). A guideline of selecting and reporting intraclass
432 correlation coefficients for reliability research. *Journal of Chiropractic Medicine*, 15,
433 155–163. doi: 10.1016/j.jcm.2016.02.012
- 434 Laffey, P. A., Peyster, R. G., Nathan, R., Haskin, M. E., & McGinley, J. A. (1984).
435 Computed tomography and aging: Results in a normal elderly population.
436 *Neuroradiology*, 26, 273–278. doi: 10.1007/BF00339770
- 437 Lamont, A. J., Mortby, M. E., Anstey, K. J., Sachdev, P. S., & Cherbuin, N. (2014). Using
438 sulcal and gyral measures of brain structure to investigate benefits of an active
439 lifestyle. *NeuroImage*, 91, 353–359. doi: 10.1016/j.neuroimage.2014.01.008
- 440 Largen, J. W., Smith, R. C., Calderon, M., Baumgartner, R., Lu, R. B., Schoolar, J. C., &
441 Ravichandran, G. K. (1984). Abnormalities of brain structure and density in
442 schizophrenia. *Biological Psychiatry*, 19, 991–1013.
- 443 Le Goualher, G., Barillot, C., Bizais, Y. J., & Scarabin, J.-M. (1996). Three-dimensional
444 segmentation of cortical sulci using active models. In M. H. Loew &
445 K. M. Hanson (Eds.), *Medical imaging 1996: Image processing*. SPIE. doi:
446 10.1117/12.237928
- 447 Le Goualher, G., Collins, D. L., Barillot, C., & Evans, A. C. (1998). Automatic
448 identificaion of cortical sulci using a 3d probabilistic atlas. In *Medical image*
449 *computing and computer-assisted intervention – MICCAI’98* (pp. 509–518). Springer
450 Berlin Heidelberg. doi: 10.1007/bfb0056236

- 451 Lee, J. K., Lee, J.-M., Kim, J. S., Kim, I. Y., Evans, A. C., & Kim, S. I. (2006). A novel
452 quantitative cross-validation of different cortical surface reconstruction
453 algorithms using MRI phantom. *NeuroImage*, *31*, 572–584. doi:
454 10.1016/j.neuroimage.2005.12.044
- 455 Lemaitre, H., Goldman, A. L., Sambataro, F., Verchinski, B. A., Meyer-Lindenberg, A.,
456 Weinberger, D. R., & Mattay, V. S. (2012). Normal age-related brain
457 morphometric changes: nonuniformity across cortical thickness, surface area and
458 gray matter volume? *Neurobiology of Aging*, *33*, 617.e1–617.e9. doi:
459 10.1016/j.neurobiolaging.2010.07.013
- 460 Leong, R. L., Lo, J. C., Sim, S. K., Zheng, H., Tandi, J., Zhou, J., & Chee, M. W. (2017).
461 Longitudinal brain structure and cognitive changes over 8 years in an east asian
462 cohort. *NeuroImage*, *147*, 852–860. doi: 10.1016/j.neuroimage.2016.10.016
- 463 Li, G., Liu, T., Nie, J., Guo, L., & Wong, S. T. C. (2008). A novel method for cortical
464 sulcal fundi extraction. In *Medical image computing and computer-assisted
465 intervention–MICCAI 2008* (pp. 270–278). Springer Berlin Heidelberg. doi:
466 10.1007/978-3-540-85988-8_33
- 467 Liu, T., Lipnicki, D. M., Zhu, W., Tao, D., Zhang, C., Cui, Y., ... Wen, W. (2012). Cortical
468 gyrification and sulcal spans in early stage Alzheimer's disease. *PLOS ONE*, *7*,
469 e31083. doi: 10.1371/journal.pone.0031083
- 470 Liu, T., Sachdev, P. S., Lipnicki, D. M., Jiang, J., Geng, G., Zhu, W., ... Wen, W. (2013).
471 Limited relationships between two-year changes in sulcal morphology and other
472 common neuroimaging indices in the elderly. *NeuroImage*, *83*, 12–17. doi:
473 10.1016/j.neuroimage.2013.06.058
- 474 Liu, T., Wen, W., Zhu, W., Kochan, N. A., Trollor, J. N., Reppermund, S., ... Sachdev,
475 P. S. (2011). The relationship between cortical sulcal variability and cognitive
476 performance in the elderly. *NeuroImage*, *56*, 865–873. doi:
477 10.1016/j.neuroimage.2011.03.015
- 478 Liu, T., Wen, W., Zhu, W., Trollor, J., Reppermund, S., Crawford, J., ... Sachdev, P.
479 (2010). The effects of age and sex on cortical sulci in the elderly. *NeuroImage*, *51*,

- 480 19–27. doi: 10.1016/j.neuroimage.2010.02.016
- 481 Lohmann, G., & von Cramon, D. Y. (2000). Automatic labelling of the human cortical
482 surface using sulcal basins. *Medical Image Analysis*, 4, 179–188. doi:
483 10.1016/s1361-8415(00)00024-4
- 484 Lohmann, G., von Cramon, D. Y., & Colchester, A. C. F. (2008). Deep sulcal landmarks
485 provide an organizing framework for human cortical folding. *Cerebral Cortex*, 18,
486 1415–1420. doi: 10.1093/cercor/bhm174
- 487 Madan, C. R. (2017). Advances in studying brain morphology: The benefits of
488 open-access data. *Frontiers in Human Neuroscience*, 11, 405. doi:
489 10.3389/fnhum.2017.00405
- 490 Madan, C. R. (2018a). Age differences in head motion and estimates of cortical
491 morphology. *PeerJ*, 6, e5176.
- 492 Madan, C. R. (2018b). Shape-related characteristics of age-related differences in
493 subcortical structures. *Aging & Mental Health*. doi:
494 10.1080/13607863.2017.1421613
- 495 Madan, C. R., & Kensinger, E. A. (2016). Cortical complexity as a measure of
496 age-related brain atrophy. *NeuroImage*, 134, 617–629. doi:
497 10.1016/j.neuroimage.2016.04.029
- 498 Madan, C. R., & Kensinger, E. A. (2017a). Age-related differences in the structural
499 complexity of subcortical and ventricular structures. *Neurobiology of Aging*, 50,
500 87–95. doi: 10.1016/j.neurobiolaging.2016.10.023
- 501 Madan, C. R., & Kensinger, E. A. (2017b). Test–retest reliability of brain morphology
502 estimates. *Brain Informatics*, 4, 107–121. doi: 10.1007/s40708-016-0060-4
- 503 Madan, C. R., & Kensinger, E. A. (2018). Predicting age from cortical structure across
504 the lifespan. *European Journal of Neuroscience*, 47, 399–416. doi: 10.1111/ejn.13835
- 505 Mangin, J.-F., Riviere, D., Cachia, A., Duchesnay, E., Cointepas, Y.,
506 Papadopoulos-Orfanos, D., ... Regis, J. (2004). Object-based morphometry of the
507 cerebral cortex. *IEEE Transactions on Medical Imaging*, 23, 968–982. doi:
508 10.1109/tmi.2004.831204

- 509 Mangin, J.-F., Rivière, D., Coulon, O., Poupon, C., Cachia, A., Cointepas, Y., ...
510 Papadopoulos-Orfanos, D. (2004). Coordinate-based versus structural
511 approaches to brain image analysis. *Artificial Intelligence in Medicine*, *30*, 177–197.
512 doi: 10.1016/s0933-3657(03)00064-2
- 513 Marcus, D. S., Wang, T. H., Parker, J., Csernansky, J. G., Morris, J. C., & Buckner, R. L.
514 (2007). Open Access Series of Imaging Studies (OASIS): Cross-sectional MRI data
515 in young, middle aged, nondemented, and demented older adults. *Journal of*
516 *Cognitive Neuroscience*, *19*, 1498–1507. doi: 10.1162/jocn.2007.19.9.1498
- 517 McGraw, K. O., & Wong, S. P. (1996). Forming inferences about some intraclass
518 correlation coefficients. *Psychological Methods*, *1*, 30–46. doi:
519 10.1037/1082-989x.1.1.30
- 520 McKay, D. R., Knowles, E. E. M., Winkler, A. A. M., Sprooten, E., Kochunov, P., Olvera,
521 R. L., ... Glahn, D. C. (2014). Influence of age, sex and genetic factors on the
522 human brain. *Brain Imaging and Behavior*, *8*, 143–152. doi:
523 10.1007/s11682-013-9277-5
- 524 Mennes, M., Biswal, B. B., Castellanos, F. X., & Milham, M. P. (2013). Making data
525 sharing work: The FCP/INDI experience. *NeuroImage*, *82*, 683–691. doi:
526 10.1016/j.neuroimage.2012.10.064
- 527 Mikhael, S., Hoogendoorn, C., Valdes-Hernandez, M., & Pernet, C. (2018). A critical
528 analysis of neuroanatomical software protocols reveals clinically relevant
529 differences in parcellation schemes. *NeuroImage*, *170*, 348–364. doi:
530 10.1016/j.neuroimage.2017.02.082
- 531 Ming, J., Harms, M. P., Morris, J. C., Beg, M. F., & Wang, L. (2015). Integrated cortical
532 structural marker for Alzheimer's disease. *Neurobiology of Aging*, *36*, S53–S59. doi:
533 10.1016/j.neurobiolaging.2014.03.042
- 534 Nowinski, W. L., Raphel, J. K., & Nguyen, B. T. (1996). Atlas-based identification of
535 cortical sulci. In Y. Kim (Ed.), *Medical imaging 1996: Image display*. SPIE. doi:
536 10.1117/12.238488
- 537 Oguz, I., Cates, J., Fletcher, T., Whitaker, R., Cool, D., Aylward, S., & Styner, M. (2008).

- 538 Cortical correspondence using entropy-based particle systems and local features.
539 In *2008 5th IEEE International Symposium on Biomedical Imaging: From nano to*
540 *macro*. IEEE. doi: 10.1109/isbi.2008.4541327
- 541 Ono, M., Kubick, S., & Abernathy, C. D. (1990). *Atlas of the cerebral sulci*. Thieme.
- 542 Palaniyappan, L., Park, B., Balain, V., Dangi, R., & Liddle, P. (2015). Abnormalities in
543 structural covariance of cortical gyrification in schizophrenia. *Brain Structure and*
544 *Function*, 220, 2059–2071. doi: 10.1007/s00429-014-0772-2
- 545 Pasquier, F., Leys, D., Weerts, J. G., Mounier-Vehier, F., Barkhof, F., & Scheltens, P.
546 (1996). Inter-and intraobserver reproducibility of cerebral atrophy assessment on
547 MRI scans with hemispheric infarcts. *European Neurology*, 36, 268–272. doi:
548 10.1159/000117270
- 549 Perrot, M., Rivière, D., & Mangin, J.-F. (2011). Cortical sulci recognition and spatial
550 normalization. *Medical Image Analysis*, 15, 529–550. doi:
551 10.1016/j.media.2011.02.008
- 552 Pizzagalli, F., Auzias, G., Kochunov, P., Faskowitz, J. I., Thompson, P. M., & Jahanshad,
553 N. (2017). The core genetic network underlying sulcal morphometry. In
554 E. Romero, N. Lepore, J. Brieva, & I. Larrabide (Eds.), *12th international symposium*
555 *on medical information processing and analysis*. SPIE. doi: 10.1117/12.2256959
- 556 Plocharski, M., & Østergaard, L. R. (2016). Extraction of sulcal medial surface and
557 classification of Alzheimer’s disease using sulcal features. *Computer Methods and*
558 *Programs in Biomedicine*, 133, 35–44. doi: 10.1016/j.cmpb.2016.05.009
- 559 Rajaratnam, N. (1960). Reliability formulas for independent decision data when
560 reliability data are matched. *Psychometrika*, 25, 261–271. doi: 10.1007/bf02289730
- 561 Reiner, P., Jouvent, E., Duchesnay, E., Cuingnet, R., Mangin, J.-F., & Chabriat, H. (2012).
562 Sulcal span in Alzheimer’s disease, amnesic mild cognitive impairment, and
563 healthy controls. *Journal of Alzheimer’s Disease*, 29, 605–613. doi:
564 10.3233/JAD-2012-111622
- 565 Rieder, R. O., Donnelly, E. F., Herdt, J. R., & Waldman, I. N. (1979). Sulcal prominence
566 in young chronic schizophrenic patients: CT scan findings associated with

- 567 impairment on neuropsychological tests. *Psychiatry Research*, 1, 1–8. doi:
568 10.1016/0165-1781(79)90021-0
- 569 Rivièrè, D., Mangin, J.-F., Papadopoulos-Orfanos, D., Martinez, J.-M., Frouin, V., &
570 Régis, J. (2002). Automatic recognition of cortical sulci of the human brain using
571 a congregation of neural networks. *Medical Image Analysis*, 6, 77–92. doi:
572 10.1016/s1361-8415(02)00052-x
- 573 Royackkers, N., Desvignes, M., Fawal, H., & Revenu, M. (1999). Detection and
574 statistical analysis of human cortical sulci. *NeuroImage*, 10, 625–641. doi:
575 10.1006/nimg.1999.0512
- 576 Salat, D. H., Buckner, R. L., Snyder, A. Z., Greve, D. N., Desikan, R. S. R., Busa, E., . . .
577 Fischl, B. (2004). Thinning of the cerebral cortex in aging. *Cerebral Cortex*, 14,
578 721–730. doi: 10.1093/cercor/bhh032
- 579 Schaer, M., Cuadra, M. B., Schmansky, N., Fischl, B., Thiran, J.-P., & Eliez, S. (2012).
580 How to measure cortical folding from MR images: A step-by-step tutorial to
581 compute local gyrification index. *Journal of Visualized Experiments*, e3417. doi:
582 10.3791/3417
- 583 Scheltens, P., Pasquier, F., Weerts, J. G., Barkhof, F., & Leys, D. (1997). Qualitative
584 assessment of cerebral atrophy on MRI: Inter- and intra-observer reproducibility
585 in dementia and normal aging. *European Neurology*, 37, 95–99. doi:
586 10.1159/000117417
- 587 Shrout, P. E., & Fleiss, J. L. (1979). Intraclass correlations: Uses in assessing rater
588 reliability. *Psychological Bulletin*, 86, 420–428. doi: 10.1037/0033-2909.86.2.420
- 589 Sowell, E. R., Peterson, B. S., Kan, E., Woods, R. P., Yoshii, J., Bansal, R., . . . Toga, A. W.
590 (2007). Sex differences in cortical thickness mapped in 176 healthy individuals
591 between 7 and 87 years of age. *Cerebral Cortex*, 17, 1550–1560. doi:
592 10.1093/cercor/bhl066
- 593 Sowell, E. R., Peterson, B. S., Thompson, P. M., Welcome, S. E., Henkenius, A. L., &
594 Toga, A. W. (2003). Mapping cortical change across the human life span. *Nature*
595 *Neuroscience*, 6, 309–315. doi: 10.1038/nn1008

- 596 Tang, Y., Hojatkashani, C., Dinov, I. D., Sun, B., Fan, L., Lin, X., . . . Toga, A. W. (2010).
597 The construction of a chinese MRI brain atlas: A morphometric comparison study
598 between chinese and caucasian cohorts. *NeuroImage*, *51*, 33–41. doi:
599 10.1016/j.neuroimage.2010.01.111
- 600 Thompson, P. M., Schwartz, C., Lin, R. T., Khan, A. A., & Toga, A. W. (1996).
601 Three-dimensional statistical analysis of sulcal variability in the human brain.
602 *Journal of Neuroscience*, *16*, 4261–4274. doi: 10.1523/jneurosci.16-13-04261.1996
- 603 Tomlinson, B., Blessed, G., & Roth, M. (1968). Observations on the brains of
604 non-demented old people. *Journal of the Neurological Sciences*, *7*, 331–356. doi:
605 10.1016/0022-510x(68)90154-8
- 606 Vaillant, M., & Davatzikos, C. (1997). Finding parametric representations of the cortical
607 sulci using an active contour model. *Medical Image Analysis*, *1*, 295–315. doi:
608 10.1016/s1361-8415(97)85003-7
- 609 Walhovd, K. B., Westlye, L. T., Amlien, I., Espeseth, T., Reinvang, I., Raz, N., . . . Fjell,
610 A. M. (2011). Consistent neuroanatomical age-related volume differences across
611 multiple samples. *Neurobiology of Aging*, *32*, 916–932. doi:
612 10.1016/j.neurobiolaging.2009.05.013
- 613 Wei, D., Zhuang, K., Ai, L., Chen, Q., Yang, W., Liu, W., . . . Qiu, J. (2018). Structural
614 and functional brain scans from the cross-sectional southwest university adult
615 lifespan dataset. *Scientific Data*, *5*, 180134. doi: 10.1038/sdata.2018.134
- 616 Welker, W. (1990). Why does cerebral cortex fissure and fold? In E. G. Jones &
617 A. Peters (Eds.), *Cerebral cortex* (Vol. 8B, pp. 3–136). Springer US. doi:
618 10.1007/978-1-4615-3824-0_1
- 619 Yue, N. C., Arnold, A. M., Longstreth, W. T., Elster, A. D., Jungreis, C. A., O'Leary,
620 D. H., . . . Bryan, R. N. (1997). Sulcal, ventricular, and white matter changes at
621 MR imaging in the aging brain: Data from the cardiovascular health study.
622 *Radiology*, *202*, 33–39. doi: 10.1148/radiology.202.1.8988189
- 623 Yun, H. J., Im, K., Yang, J.-J., Yoon, U., & Lee, J.-M. (2013). Automated sulcal depth
624 measurement on cortical surface reflecting geometrical properties of sulci. *PLOS*

625 *ONE*, 8, e55977. doi: 10.1371/journal.pone.0055977
626 Zuo, X.-N., Anderson, J. S., Bellec, P., Birn, R. M., Biswal, B. B., Blautzik, J., ... Milham,
627 M. P. (2014). An open science resource for establishing reliability and
628 reproducibility in functional connectomics. *Scientific Data*, 1, 140049. doi:
629 10.1038/sdata.2014.49